13th World Conference on Earthquake Engineering
Vancouver, B.C., Canada
August 1-6, 2004
Paper No. 1258

A STUDY ON CHARACTERISTICS OF RUBBER BEARINGS CONSIDERING ROTATION ANGLE AND COMPRESSIVE FORCE DEPENDENCE

Takafumi MIYAMA [1], Keiji MASUDA [2], Demin FENG [3]

SUMMARY

Base-isolated buildings with high aspect ratios are becoming increasingly popular. For those buildings, the rubber bearings must bear large axial stress, large fluctuation of axial stress and large horizontal deformation. When the isolation systems are installed in the middle level of structure, the effects of rotation deformation must be taken into account. In this paper, a simple mechanical model is proposed to include the effects of axial stress, horizontal deformation as well as many other things on rotational and horizontal stiffness. The expression of the vertical deformation of rubber bearings is theoretically introduced considering the rotation effect. The dependence of shear deformation on axial stiffness and dependence of axial force on shear stiffness are evaluated. It was confirmed that the results of proposed model agree well with the experimental results, through the static loading test of rubber bearings and the shaking table test of base-isolated building with high aspect ratios. We also found that careful attention to the influence of vertical vibration on the development of a large axial force and deformation is required. This is caused in connection with horizontal, vertical and rocking vibration.

INTRODUCTION

Base isolation buildings with high rise and high aspect ratios are becoming increasingly popular. For those buildings, the rubber bearings must bear large axial stress because the natural period of these buildings is long. Also, fluctuations in axial stress become large because the rocking moment is large. The top and bottom ends of rubber bearings are fixed to the rotation of a conventional base isolation building. Many tests of the rubber bearing have been conducted with the rotation-fixed condition. The extreme case of the effects by axial force and rotation has been considered in the conventional design. However, the detailed case is not considered. Large axial stress, fluctuation in axial stress, large horizontal strain and large rotation has not been required in the design for these base isolation buildings.
Buildings installed base isolation system in the middle level of a structure or the gap between piles and basements are required to reduce the construction cost. For these buildings, the effects of rotation deformation in the top/bottom end of the rubber bearing must be taken into account.

---

[1] Chief Researcher, Fujita Corporation, Tokyo, Japan. Email: miyama@fujita.co.jp
[2] Chief Engineer, Fujita Corporation, Tokyo, Japan. Email: kmasuda@fujita.co.jp
[3] Chief Researcher, Fujita Corporation. Kanagawa, Japan. Email: feng@ fujita.co.jp

We have conducted tests on rubber bearings to investigate the effects of rotation, axial stress and large horizontal deformation. In this paper, a simple model is proposed to account for the effects of axial stress, horizontal deformation and as well as other things on rotational and horizontal stiffness. The dependency is evaluated from test results and theoretical values. The vertical deformation is theoretically obtained in the case where rotation is considered. The theoretical value is verified by the test results. The dynamic response analysis is conducted using a proposed model and verified by the shaking table test of high rise isolated building.

PREVIOUS THEORETICAL RESEARCH ON THE RUBBER BEARING

The Horizontal Stiffness of the rubber bearing

Fig.1 shows a rubber bearing supporting a vertical force P, a shear force Q and a bending moment M. Its mechanical characteristics were described by Haringx[1,2,3]. The balance of forces are given in a form of differential Eq.(1) and Eq.(2).

$$M(z) = k_{rc}\frac{d\theta}{dz} = -M_B - Px + Q_B Z \tag{1}$$

$$Q(z) = k_s\gamma_s = k_s\left(\frac{dx}{dz} - \theta\right) = -Q_B + P\theta \tag{2}$$

The symbol γ_s is a nominal shear strain after subtracting the bending rotation from the shear strain γ. The shear strain γ is the quotient that the horizontal deformation is divided by the total of rubber sheets height. Eq.(3) and Eq.(4) are obtained by solving the Eq.(1) and Eq.(2).

$$x(z) = C_1\sin(qz) + C_2\cos(qz) + \frac{-M_B}{P} + \frac{Q_B}{P}z \tag{3}$$

$$\theta(z) = \frac{P}{q^2 k_{rc}}\left(C_1 q\cos(qz) - C_2 q\sin(qz)\right) + \frac{Q_B}{P} \tag{4}$$

Where,

$$k_{rc} = \frac{E_{rb}Ih}{nt_r},\quad k_s = \frac{GAh}{nt_r},\quad q = \sqrt{\frac{P}{k_{rc}}\left(1 + \frac{P}{k_s}\right)}$$

And the symbol nt_r shows the total height of rubber sheets (n:layers $\times$ t_r :thickness), h is the total height of rubber and steel plates, G shows the shear modulus, E_{rb} shows the bending modulus corrected by the volume modulus, I shows the geometrical moment of inertia and A shows the area.

The horizontal stiffness of the rubber bearing K_h is obtained under the boundary condition that the bottom end is fixed $(x(0) = \theta(0) = 0)$, the rotation of the top end is fixed $(\theta(h) = 0)$ and the shear force is $F = Q_A = -Q_B$.

$$K_h = \frac{P^2}{\left(2k_{rc}q\tan\frac{qh}{2} - Ph\right)} \tag{5}$$

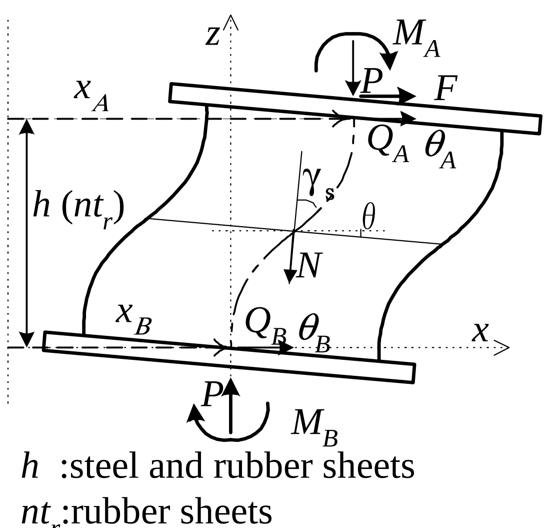

Fig.1 Rubber Bearing

The buckling load is given when the denominator of Eq.(5) becomes infinity, and it is approximated by Eq.(6).

$$P_{cr} = \frac{\pi P}{hq} = \frac{\pi}{h}\sqrt{k_s k_{rc}} \tag{6}$$

Eq.(5) can be approximately expressed in Eq.(7) by using Eq.(6).

$$K_h = \frac{k_s}{h}\left\{1 - \left(\frac{P}{P_{cr}}\right)^2\right\} \tag{7}$$

The stiffness matrix of horizontal deformation and rotation components

Iizuka[4] derived stiffness matrix, shown in Eq.(8), by using Eq.(3), and Eq.(4). The rotation stiffness and the geometrical non-linearity are considered in this equation.

$$\begin{Bmatrix} Q_A \\ M_A \\ Q_B \\ M_B \end{Bmatrix} = K_h \begin{bmatrix} k_1 & k_2 & -k_1 & k_2 \\ & k_3 & -k_2 & k_4 \\ & & k_1 & -k_2 \\ & sym. & & k_3 \end{bmatrix} \begin{Bmatrix} x_A \\ \theta_A \\ x_B \\ \theta_B \end{Bmatrix} \tag{8}$$

Where,

$$k_1 = 1, \quad k_2 = -\frac{k_{rc} q}{P}\tan\left(\frac{qh}{2}\right)$$

$$k_3 = \frac{k_{rc} q}{K_h \tan(qh)} + \left(\frac{k_{rc} q}{P}\tan\left(\frac{qh}{2}\right)\right)^2 \quad 2$$

$$k_4 = -\frac{k_{rc} q}{K_h \sin(qh)} + \left(\frac{k_{rc} q}{P}\tan\left(\frac{qh}{2}\right)\right)^2$$

The components in the matrix are shown with trigonometrical functions of axial force, horizontal stiffness and bending stiffness. It is difficult to clarify the mutual effects of components and axial force. It is also difficult to deal with the material nonlinearity such as the hardening caused by large deformation or the yielding by the tension force.

Vertical deformation caused by horizontal and rotation deformation

The vertical deformation of the rubber bearing δ_c shown in Eq.(9) is obtained as the sum of the geometrical deformation δ_{c1} caused by bending-shear deformation and the axial deformation δ_{c2} caused by axial strain. δ_{c1} is divided into $\delta_{c1\theta=0}$, which is the vertical deformation when the rotation of the top and bottom end is 0, and $\delta_{c1\theta}$, which is the deformation caused by the rotation of both ends. In the same manner, δ_{c2} is divided into $\delta_{c2\theta=0}$ and $\delta_{c2\theta}$. $\delta_{c2\theta=0}$ is also divided into Pnt_r / AE_{cb} , which is the deformation when the shear deformation is 0, and $\delta'_{c2\theta=0}$, which is the deformation caused by the shear deformation.

$$\begin{aligned} \delta_c &= \delta_{c1} + \delta_{c2} \\ &= \left(\delta_{c1\theta=0} + \delta_{c1\theta}\right) + \left(\delta_{c2\theta=0} + \delta_{c2\theta}\right) \\ &= \left(\delta_{c1\theta=0} + \delta_{c1\theta}\right) + \left(\frac{Pnt_r}{AE_{cb}} + \delta'_{c2\theta=0} + \delta_{c2\theta}\right) \end{aligned} \tag{9}$$

Fuller[5] deduced the vertical deformation, shown in Eq.(10) caused by bending-shear deformation based on Eq.(1) and Eq.(2) , when the rotations of both ends are 0.

$$\delta_{c1\theta=0} = \frac{(nt_r\gamma)^2\beta^2\left[\frac{\zeta}{2}\left\{\left(1+\tan^2\frac{\zeta}{2}\right)(1+2\beta)+2\right\}-(3+2\beta)\tan\frac{\zeta}{2}\right]}{2h\zeta\left(2\alpha\zeta\tan\frac{\zeta}{2}-\beta^2\right)} \tag{10}$$

Where

$$\alpha = \frac{1}{\pi^2}\frac{Ant_r\sigma_{cr}}{AhG}\left(1+\frac{Ant_r\sigma_{cr}}{AhG}\right) = \frac{1}{\pi^2}\frac{P_{cr}}{k_s}\left(1+\frac{P_{cr}}{k_s}\right) = \frac{k_{rc}}{h^2k_s}\ ,\ \ \beta = \frac{Ant_r\sigma}{AhG} = \frac{P}{k_s}$$

$$\zeta = \sqrt{\frac{\beta(1+\beta)}{\alpha}} = \sqrt{\frac{P}{k_s}\left(1+\frac{P}{k_s}\right)\frac{h^2k_s}{k_{rc}}} = qh$$

Uryu[6] deduced the vertical deformation of which result is same to Eq.(10). He also made an approximation with the Taylor series shown in Eq.(11).

$$\delta_{c1\theta=0} = \frac{Pnt_r}{A}\cdot\frac{F^2h^2}{12k_{rc}k_sG}\cdot\frac{P+k_s}{P} \tag{11}$$

He then obtained the vertical deformation caused by axial force shown in Eq.(12), when the rotations of both sides are fixed to 0.

$$\delta_{c2\theta=0} = \frac{1}{AE_{cb}}\left[Pnt_r + \frac{F^2h}{P}\left(1-\frac{\tan\left(\frac{qh}{2}\right)}{\frac{qh}{2}}\right)+\frac{3F^4h}{4P^3}\left(1-\frac{\tan\left(\frac{qh}{2}\right)}{\frac{qh}{2}}+\frac{\tan^2\left(\frac{qh}{2}\right)}{3}\right)\right] \tag{12}$$

He applied the Taylor series to Eq.(12) regarding P/k_s as very large. He obtained Eq.(13).

$$\delta_{c2\theta=0} = \frac{Pnt_r}{AE_{cb}}\left(1-\frac{k_s}{A}\cdot\frac{F^2h^2}{12k_{rc}k_sG}\cdot\frac{P+k_s}{P}\right) \tag{13}$$

Those equations show the deformation when the rotation of both ends of rubber bearing are fixed. When the both ends rotate, the vertical deformation has not yet been shown.

A PROPOSAL OF NEW MODEL FOR RUBBER BEARINGS TO EVALUATE THE VARIETY OF DEPENDENCE

Proposed model

The new model shown in Fig.2 is proposed to deal with rotation and horizontal deformation at the same time and also to deal with non-linearity of material and variety of dependence, such as axial pressure dependence or horizontal deformation dependence. Horizontal spring and rotation spring, which are aggregating the characteristics of rubber bearings, are installed in the intermediate height and are connected by two rigid bars. The nonlinearity and dependence is easily accounted for using those springs. The equation of equilibrium is shown in Eq.(14).

$$\begin{Bmatrix} Q_A \\ M_A \\ Q_B \\ M_B \end{Bmatrix} = [\mathrm{K}_H + \mathrm{K}_P + \mathrm{K}_R]\begin{Bmatrix} x_A \\ \theta_A \\ x_B \\ \theta_B \end{Bmatrix}$$

$$= \left[K_h^* \begin{bmatrix} 1 & -h/2 & -1 & -h/2 \\ & h^2/4 & h/2 & h^2/4 \\ & & 1 & h/2 \\ sym. & & & h^2/4 \end{bmatrix} + P \begin{bmatrix} 0 & -1/2 & 0 & -1/2 \\ & h/4 & 1/2 & h/4 \\ & & 0 & 1/2 \\ sym. & & & h/4 \end{bmatrix} + K_r^* \begin{bmatrix} 0 & 0 & 0 & 0 \\ & 1 & 0 & -1 \\ & & 0 & 0 \\ sym. & & & 1 \end{bmatrix} \right] \begin{Bmatrix} x_A \\ \theta_A \\ x_B \\ \theta_B \end{Bmatrix} \quad (14)$$

Comparing Eq.(14) to Eq.(8), the stiffness of two springs in the elastic range are obtained in Eq.(15) and Eq.(16).

$$K_h^* = K_h \quad (15)$$

$$K_r^* = \frac{k_{rc}}{h} \cdot \frac{\frac{qh}{2}}{\tan \frac{qh}{2}} \quad (16)$$

The matrix $[\mathrm{K}_H]$ indicates the bending-shear. It is represented by the well-known horizontal stiffness K_h. The matrix $[\mathrm{K}_P]$ indicates the secondary moment $P\Delta$ and the shear force caused by it. The matrix $[\mathrm{K}_R]$ indicates the uniform moment and shear force caused by the rotation of top or bottom end. The stiffness K_r^* is the rotational stiffness installed at an intermediate height.

The effects of axial force

In the elastic range, the horizontal stiffness K_h^* is same as Eq.(5). Accordingly the effect of axial force is also shown in Eq.(7). And the effects of the axial force on rotation stiffness K_r^* is as same as horizontal stiffness in the elastic range. The effect of axial force is shown in the same way in Eq.(17).

$$K_r^* = \frac{k_{rc}}{h} \left\{ 1 - \left(\frac{P}{P_{cr}} \right)^2 \right\} \quad (17)$$

THE VERTICAL DISPLACEMENT BY THE ROTATION OF THE RUBBER BEARING

The vertical deformation caused geometrically by bending-shear deformation

The infinitesimal vertical deformation $\Delta\delta_{c1}$ in the infinitesimal height Δz of the rubber bearing is shown in Eq.(18) and Fig.3. This shows the sum of vertical deformation caused by bending deformation and shear deformation.

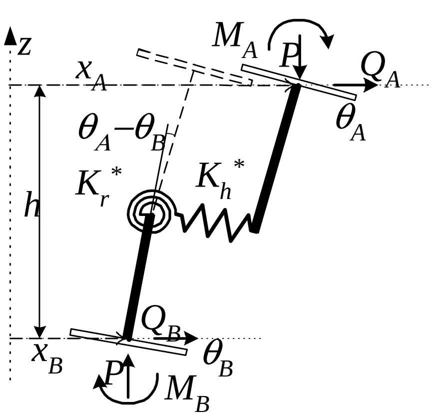

Fig.2 Proposed Model

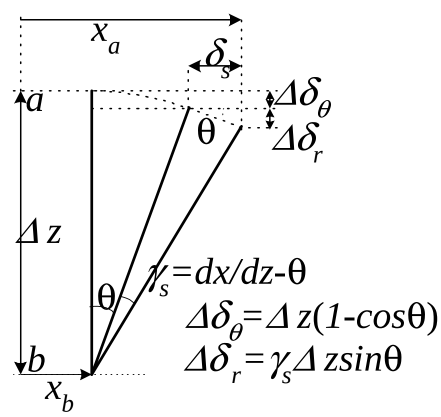

Fig.3 Vertical Deformation

$$\begin{aligned}\Delta\delta_{c1} &= \Delta z(1-\cos\theta)+\gamma_s \Delta z\sin\theta \\ &\approx \frac{dx}{dz}\theta\Delta z - \frac{1}{2}\theta^2\Delta z \end{aligned} \tag{18}$$

The boundary condition is defined as the bottom end is fixed $(x(0)=\theta(0)=0)$, and the rotation of the top end is applied $(\theta(h)=\theta_A)$. These boundary conditions are taking into the solution of a differential equation shown in Eq.(3) and Eq.(4). The results are applied to Eq.(18) and integrated over the whole height. Therefore the geometrical deformation caused by bending-shear deformation is obtained by Eq.(19).

$$\begin{aligned}\delta_{C1} &= \left(\frac{k_{rc}q^2}{P}-\frac{1}{2}\right)\left\{\left(\frac{-M_B^2}{2k_{rc}{}^2q^3}+\frac{F^2}{2qP^2}\right)\sin qh\cos qh - \frac{M_BF}{Pk_{rc}q^2}\sin^2 qh \right. \\ &\left. +\frac{h}{2}\left(\frac{M_B^2}{k_{rc}{}^2q^2}+\frac{F^2}{P^2}\right)\right\}+\frac{F}{P^2}\left\{M_B(\cos qh-1)-\frac{Fk_{rc}q}{P}\sin qh\right\}+\frac{F^2}{2P^2}h \end{aligned} \tag{19}$$

Adding the boundary condition that the rotation of the top end is fixed $(\theta(h)=0)$ and M_B being expressed by F, Eq.(19) is in agreement with Eq.(10). Eq.(11) is given by the approximation with the Taylor series from Eq.(19). Furthermore, Eq.(20) is given on the condition that the P/k_s is sufficiently larger.

$$\delta_{c1\theta=0} = \frac{\pi^2 Pnt_r G\gamma^2}{12A\sigma_{cr}^2} \tag{20}$$

The approximation of vertical deformation $\delta_{C1\theta}$ caused by the rotation θ_A of the top end is supposed to be produced by the uniform moment. The horizontal deformation δ_A is caused by θ_A is shown in Eq.(21).

$$\delta_A = 0.5h\theta_A \tag{21}$$

The approximation of vertical deformation $\delta_{C1\theta}$ caused by the rotation of the top end is obtained in Eq.(22) by integration, when the shear strain $dx/dz=\gamma$ is uniform along the height, higher order terms of small quantities are neglected, and paying attention that the total height of rubber is not h but nt_r.

$$\begin{aligned}\delta_{C1\theta} &\approx \frac{nt_r}{h}\int_0^h \frac{dx}{dz}\theta(z)dz \\ &= \frac{nt_r\gamma\theta_A}{2}\end{aligned} \tag{22}$$

The vertical deformation caused by the axial stress

The axial force N is the sum of vertical load P and the axial component of horizontal force F in Fig.1. N is shown in Eq.(23), when the $\theta(z)$ is obtained when the bottom end of the rubber bearing is fixed $(x(0)=0,\theta(0)=0)$.

$$\begin{aligned}N(x) &= P - F\theta(z) \\ &= P-\frac{F^2}{P}\cos qx+\frac{FM_B}{k_{rc}q}\sin qx+\frac{F^2}{P}\end{aligned} \tag{23}$$

The vertical deformation caused by the vertical deformation δ_{C2} is shown in Eq.(24) by integrating axial stress caused by the axial force shown in Eq.(23). In this equation, equivalent compressive stiffness E_{cb} is used, and the attention is paid to the total rubber height nt_r in the domain of integral $0\le x\le h$.

$$\delta_{c2} = \frac{nt_r}{AhE_{cb}}\int_0^h\left(P-\frac{F^2}{P}\cos qx+\frac{FM_b}{k_{rc}q}\sin qx+\frac{F^2}{P}\right)dz$$

$$= \frac{nt_r}{AhE_{cb}}\left(Ph + \frac{F^2h}{P} - \frac{F^2}{Pq}\sin qh - \frac{FM_b}{k_{rc}q^2}\cos qh + \frac{FM_b}{k_{rc}q^2}\right) \tag{24}$$

Adding the boundary condition that the rotation of the top end is fixed $(\theta(h)=0)$, M_B is expressed by F, and applying the approximation with the Taylor series as P/P_{cr} is sufficiently smaller, Eq.(24) is simplified to Eq.(25).

$$\delta_{c2\theta=0} = \frac{Pnt_r}{AE_{cb}}\left(1 - \frac{1}{12}\left(\frac{\pi G\gamma}{\sigma_{cr}}\right)^2\right) \tag{25}$$

The approximation of vertical deformation $\delta_{C2\theta}$ caused by the rotation θ_A of the top end is obtained by the uniform moment in the same manner of Eq.(22). The result is shown in Eq.(26). In this approximation, the condition that P/P_{cr} is sufficiently smaller is used. In this equation, $\delta_{C2\theta}$ is a negative value and it decreases as rotation angle θ_A or horizontal shear strain γ increases.

$$\begin{aligned}\delta_{c2\theta} &= \frac{-nt_r}{AhE_{cb}}\int_0^h F\theta(z)dz \\ &= -\frac{nt_r G\gamma\theta_A}{2E_{cb}}\end{aligned} \tag{26}$$

Eq.(20), Eq.(22), Eq.(25) and Eq.(26) are summarized as Eq.(27).

$$\delta_c = \frac{Pnt_r}{AE_{cb}} + \frac{\pi^2 Pnt_r G\gamma^2}{12A\sigma_{cr}^2}\left(1 - \frac{G}{E_{cb}}\right) + \frac{nt_r\gamma\theta}{2}\left(1 - \frac{G}{E_{cb}}\right) \tag{27}$$

Therefore, G/E_{cb} is small enough to neglect, in this equation.

APPLICATION OF PROPOSED MODEL TO THE NON-LINEAR BEHAVIOR OF THE RUBBER BEARING

The evaluation of non-linear behavior

Eq.(14) enable us to evaluate the characteristics of rubber bearing from small to large range of deformation by considering non-linearity and dependence in K_h^* and K_r^*. In this paper, axial force dependence and horizontal deformation dependence are considered. These dependencies are thought to be independent. The summarized characteristics of aggregated spring K_h^* and K_r^* are supposed to be the products of those factors as shown in Eq.(28) and Eq.(29), when the effects of axial force and horizontal deformation applied simultaneously.

$$K_h^* = \frac{k_s}{h}\varphi_h(P)\phi_h(x) \tag{28}$$

$$K_r^* = \frac{k_{rc}}{h}\varphi_r(P)\phi_{rc}(x) \tag{29}$$

Where,

$\varphi_h(P)$: Factor of dependency by the axial force to the horizontal stiffness.
$\phi_h(x)$: Factor of dependency by the horizontal deformation to the horizontal stiffness.
$\varphi_r(P)$: Factor of dependency by the axial force to the rotation stiffness.
$\phi_{rc}(x)$: Factor of dependency by the shear deformation to the rotation stiffness.

In the following chapters, The characteristics of those factors are investigated independently. It is also confirmed that the product of each dependency shown in Eq.(28) and Eq.(29) is in agreement with test result, when the axial force and horizontal deformation are applied simultaneously.

A experiment to investigate the dependence

Authors[Miyama, 7,8,9] conducted experiment to clarify the effects of rotation of the top/bottom end of the rubber bearing and the effects of axial force. Conducted experiments are as follows.

A) Rotation performance tests under the constant shear strain and vertical force
B) Vertical performance test under the constant shear strain and fixed rotation
C) Horizontal performance tests under the constant vertical force and fixed rotation
D) Horizontal performance tests under the varying vertical force and fixed rotation
E) Horizontal performance tests under the constant vertical force and varying rotation
F) Horizontal performance tests under the varying vertical force and varying rotation

The rubber bearings, which have a diameter of 300mm, the first shape factor of S_1=23.1, the second shape factor of S_2=4.8, are used in these experiments.

Case-E is supposed as the column in the center or the building. In this case, rotation is increases as the horizontal deformation increases under the constant axial force. Case-F is supposed as the outside column. In this case, axial force and rotation angle increase as the horizontal deformation increases. Fig.4 shows the loading schedule of the Case-D, Case-E and Case-F schematically. The positive rotation angle of the top end causes as the moment of the bottom end increases. From these experimental results, the dependence of each factor is clarified.

Axial stress dependence to horizontal stiffness and rotation stiffness

Axial stress dependence to horizontal stiffness is theoretically obtained as shown in Eq.(5), and is approximated by Eq.(7). In these equations, the horizontal stiffness decreases as the axial stress increases. The experimental results show the general trends of these equations. But it was pointed out that the effects differ from the manufacturing methods of rubber bearing.

Fig.5 shows the results of axial force dependence to rotation stiffness obtained from Case-E. It also shows the other test results, which are obtained from different rubber bearings with different shape factors. In these rotational performance tests, when the rotation exceeds the yield point, the stiffness becomes smaller. In this figure, elastic value and the theoretical value are shown. Those theoretical value are obtained from the top end moment and rotation angle under the condition that the bottom end is fixed and top end is rotated. This value is additionally affected by the horizontal stiffness K_h^* and axial force P, as shown in Eq.(14), but those effects are small compare with rotation stiffness K_r^*.

Because a rubber bearing has partial tension stress zone when the axial pressure is small, the rotation stiffness is very small. As the axial stress increase, the rotation stiffness increases. And it reaches the peak when the axial stress is around 3Mpa. The theoretical value is smaller than test result when the axial stress is less than 5Mpa. When the axial stress increases to more than 10Mpa, the theoretical value is almost same as the experimental results. From these results, the rotation stiffness decreases as the axial force increases when the rubber bearing doesn't have tension stress zone, and the axial force dependence is larger than the theoretical value. But considering the effects of manufacturing method, quantity of experimental results, and the theoretical value agrees well when the axial stress

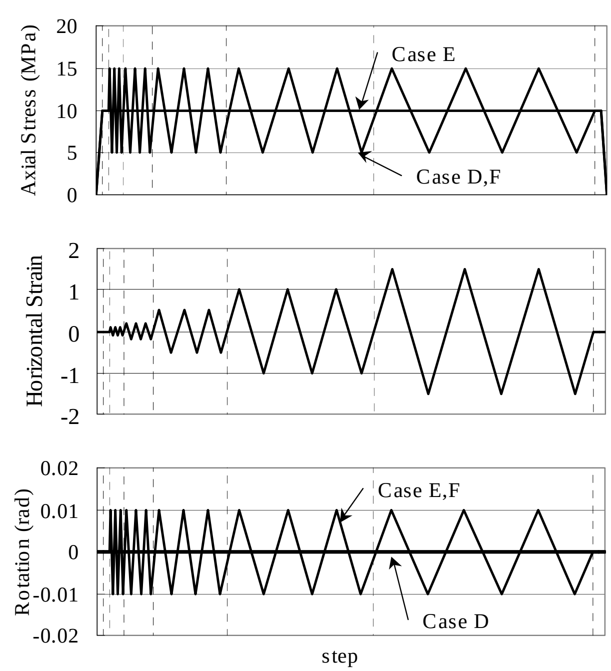

Fig.4 Loading Schedule

is larger then 10Mpa, the axial stress dependence to rotation stiffness $\varphi_r(P)$ used in Eq.(29) is defined from theoretical value shown in Eq.(17).

$$\phi_r(P) = 1 - \left(\frac{P}{P_{cr}}\right)^2 \qquad (30)$$

The horizontal deformation dependence to horizontal stiffness

The horizontal stiffness decreases as the horizontal deformation increases. Further deformation causes a hardening of stiffness or an unstable condition. These phenomena are generally evaluated from test results. The mean secant horizontal stiffness is obtained for several horizontal strain ranges. Fig.6 shows the experimental result of horizontal deformation dependence to horizontal stiffness normalized by the stiffness at 100% horizontal shear strain. Fig.6 also shows the approximation of function as described below.

$$\phi_h(x) = \left(\frac{x}{nt_r}\right)^{-0.16} \qquad (31)$$

The horizontal deformation dependence to the rotation stiffness

The former information about the horizontal deformation dependence to the rotation stiffness is limited. Fig.7 shows the test results. They show the average value of tangent stiffness in the elastic range for two specimens. It decreases as the horizontal deformation increases. They are affected by the horizontal stiffness K_h^* and axial force P, as shown in Eq.(14). But, those are neglected from the evaluation of the dependence, because they are small compared with rotational stiffness K_r^*. The decrease of the stiffness under the assumption that the second moment of overlapped area of top and bottom end shown in Eq.(32) lineally affects the rotation stiffness. It agree well with the test results.

$$\phi_{rc}(x) = \frac{4}{\pi}\left(\frac{1}{2}\theta_d + 2\theta_d \cos^2\theta_d - \frac{13}{6}\sin^3\theta_d \cos\theta_d - \frac{5}{2}\sin\theta_d \cos^3\theta_d\right) \qquad (32)$$

Where

$$\cos\theta_d = \frac{\delta}{D} \qquad (33)$$

In this figure, the axial force dependence is not clear when the horizontal deformation is large. It is considered that the dependence becomes immeasurable because the horizontal deformation dependence is larger than the axial force dependence in the test results.

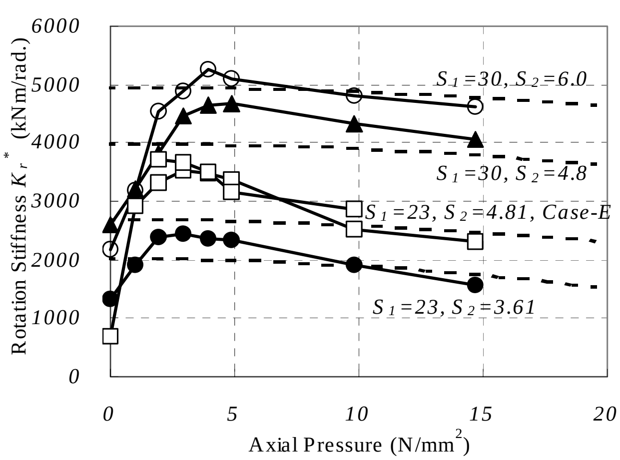

Fig.5 Loading Schedule

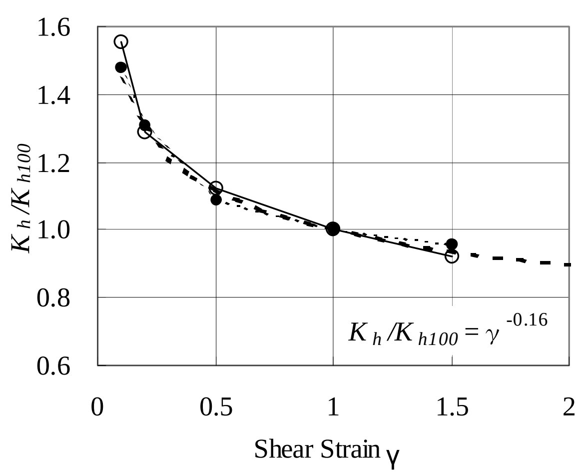

Fig.6 Horizontal Deformation Dependence

The effects of axial force and horizontal deformation applied simultaneously

To confirm that the effects of dependence are expressed by Eq.(14), when the axial force and horizontal deformation applied simultaneously, Eq.(14) is compared with the test results. The horizontal stiffness used in Eq.(14) is derived from Fig.6 when shear strain is 100% and axial stress is 10Mpa. The used rotational stiffness is the maximum value in Fig.5.

Fig.8 shows the relationship between horizontal force and horizontal deformation for the Case-F. The test results agree well with the results of Eq.(14). It shows, in the positive direction, that the horizontal force decreases, when the rotation angle and axial stress increases as the horizontal deformation increase. On the contrary, the shear force doesn't decrease because the axial force isn't small in the negative direction.

Fig.9 shows the relationship between moment and rotation angle for Case-E. Because there is some friction in the testing machine, the moment value is different between the increasing stage and the decreasing stage of the moment. The friction value is almost same along the loading and unloading. The average value can be said to be the corrected value. The moment value of the test result matches with the result of Eq.(14). In this figure, the moment increases as the rotation angle increases when the shear deformation is small. But when the shear deformation is large, the moment increases by the shear force and secondary moment $P\Delta$ even the rotation angle is small.The positive direction of the moment by the rotation is defined to be the direction that the rotation decrease moment by positive shear force. Eventually, the relationship between moment and rotation angle, when the shear strain is large, shows the negative gradient.

Fig.10 shows the relationship between horizontal force and rotation angle for the Case-E. The results of Eq.(14) matches with the test results when the shear strain is large. The decline of the stiffness is shown properly, when the shear strain is small. From those results, Eq.(14) is well agreed with the test results.

Fig.11 shows the relationship between moment and rotation angle, and Fig.12 shows the relationship between shear force and rotation angle for the Case-F. The axial force increases, when the rotation angle is positive, and vice verse in this case. Consequently, the shear force is different by the plus minus of rotation angle. In this case, the results of Eq.(14) agree well with the test results. It can be said that this equation shows the appropriate agreement and may be used for the evaluation of characteristics when the dependence is considered.

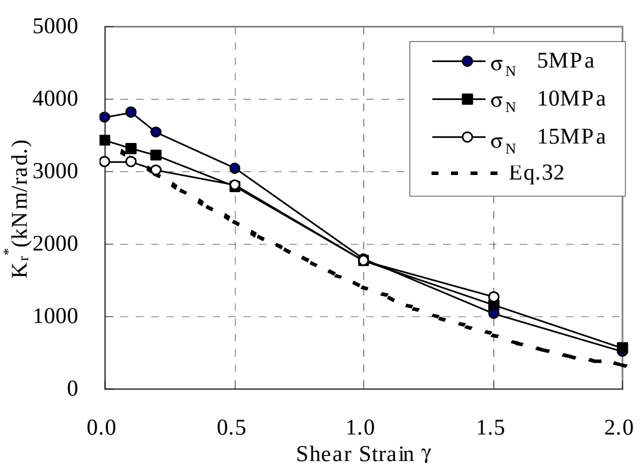

Fig.7 Horizontal Deformation Dependence

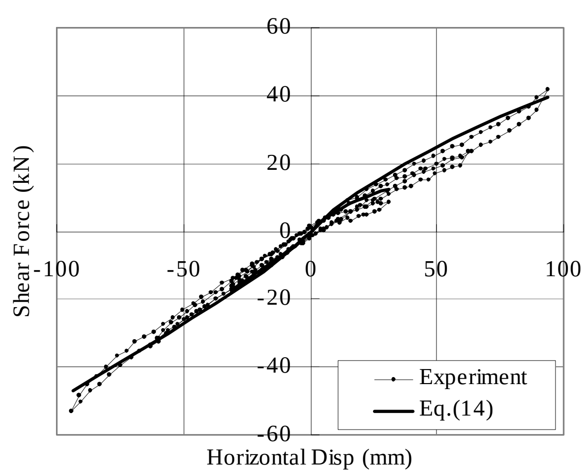

Fig.8 Axial Force Dependence

THE COMPARISON OF VERTICAL DEFORMATION BETWEEN THE TEST RESULTS AND THEORETICAL VALUE

Vertical stiffness when the rotation angle is 0

The vertical stiffness is measured by the range of 10±3Mpa for several horizontal strains. Fig.13 shows the normalized stiffness by calculating the stiffness when the shear deformation is 0. In this figure, the results of Eq.(27) and the results of an experimental equation by Fujita[10] are also shown. The longitudinal axis is also normalized by the vertical stiffness K_{v0} when the shear deformation is 0.

The vertical stiffness is greater than the result of Eq.(27) when the shear strain is greater than 200%. It is considered that the rubber bearing is affected by the hardening of rubber caused by the large horizontal deformation. The result is the intermediate value of Eq.(27) and Fujita's value when the shear strain is less than 150%. From those results, the effects of horizontal force to the vertical stiffness can be evaluated by Eq.(27).

The vertical deformation by the rotation

From the test results of Case-A, the relationship between the angle of rotation and vertical deformation is compared with the results of Eq.(27). Because attention is paid to the effects of rotation in this comparison, the effects of the axial force and/or the horizontal force are removed from the experimental results. Therefore, the experimental results are shifted to coincide with the theoretical value when the

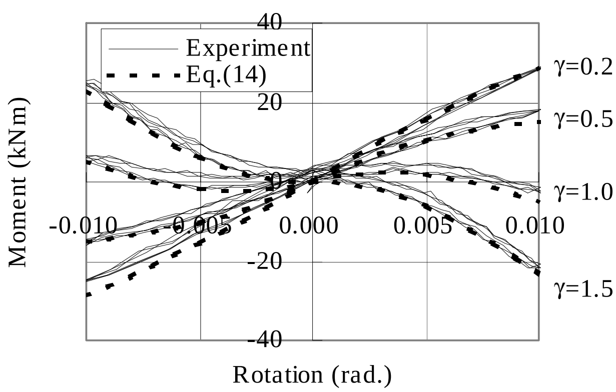

(Case-E)
Fig.9 Moment – Rotation Relation

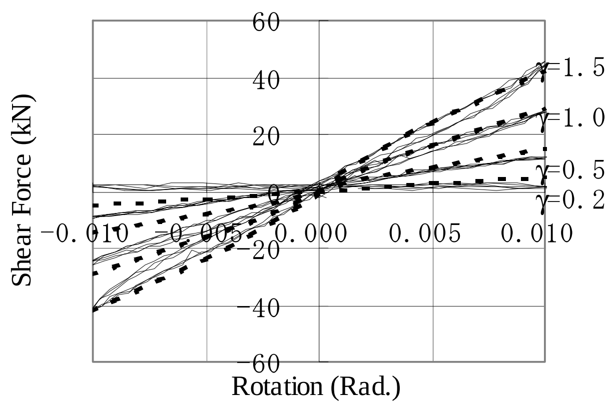

(Case-E)
Fig.10 Moment – Shear Force Relation

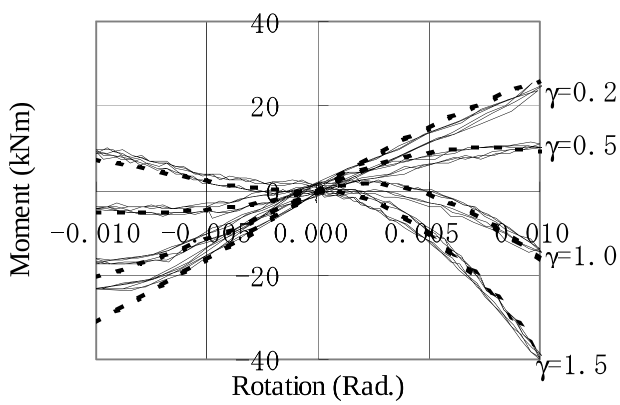

(Case-F)
Fig.11 Moment – Rotation Relation

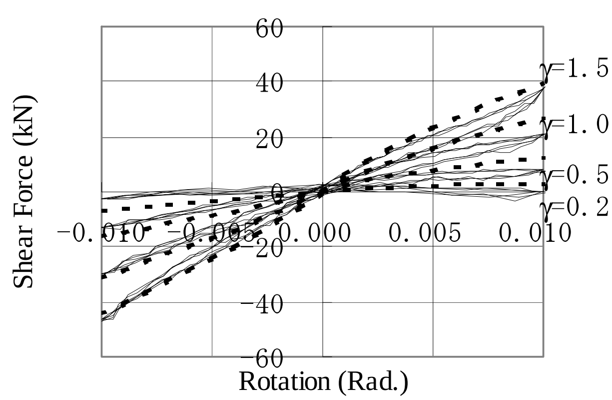

(Case-F)
Fig.12 Moment – Shear Force Relation

rotation angle is 0.

Fig.14 shows the experimental results and theoretical value. The theoretical value in case of the shear strain is 20% match the test result when the rotation angle is small. When the rotation angle is greater than 0.01rad., the vertical deformation decreases to the negative direction. This is because of the tensile yielding of the rubber. It is confirmed by the relationship between the moment and angle of rotation. When the shear deformation is large, Eq.(27) agree well with the test results. From those results, the validity of the Eq.(27) is confirmed

THE DYNAMIC RESPONSE ANALYSIS CONSIDERING DEPENDENCY

The relationship between horizontal force and horizontal deformation

The dependency of axial force and horizontal deformation are considered in Eq.(14). To examine the equation for its validity in the dynamic response analysis, shaking table test results of the isolated building are compared with the analytical results. The shaking table test is performed with a one 12th scale model that has an aspect ratio of 5, height is 4m and weight is 19t[Miyama, 11,12]. This model is supported by

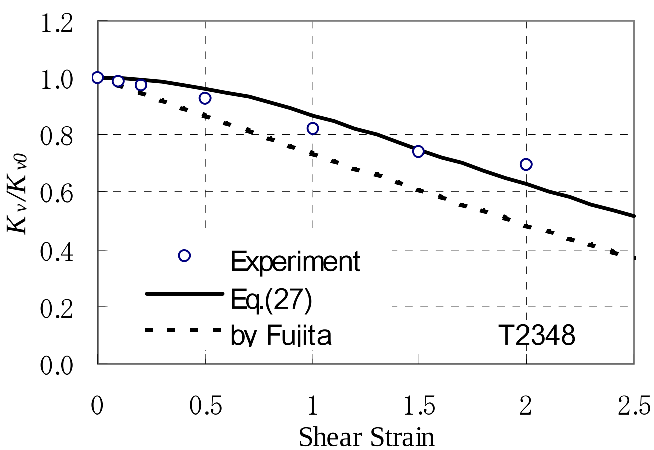

Fig.13 Vertical Stiffness

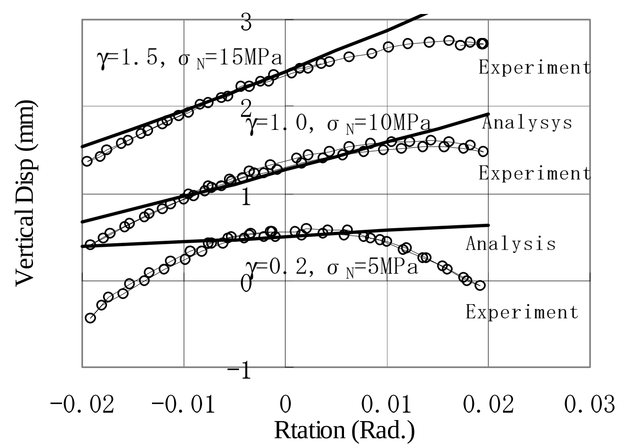

Fig.14 Vertical Deformation

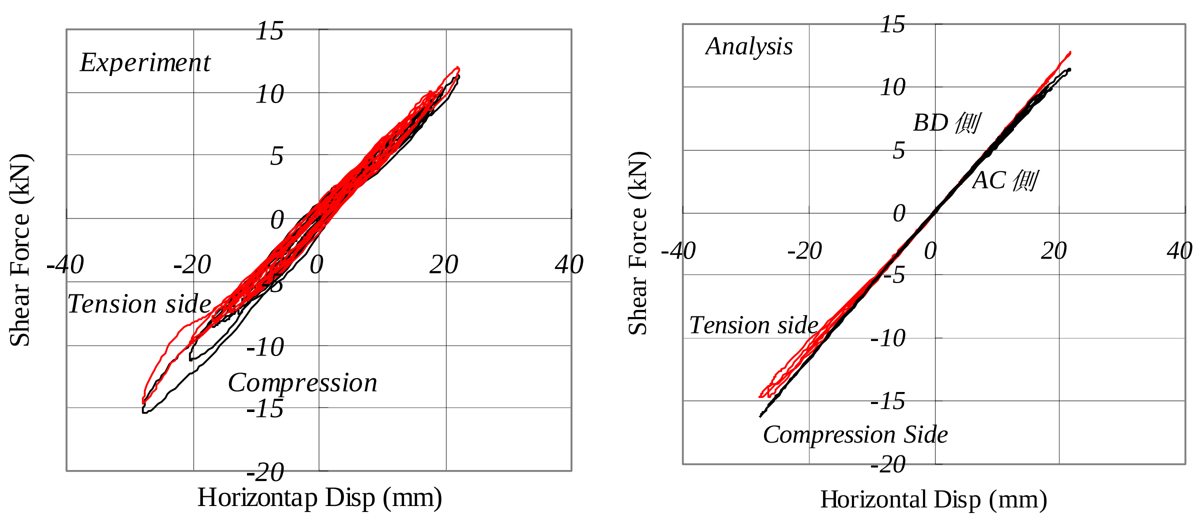

Experiment **Analysis**

Fig.15 Shear Force - Horizontal Deformation

four rubber bearings and 2 oil dampers. The damping force of those dampers is proportional to velocity. Considering the capacity of shaking table, the natural frequency is set to be a little short at the value of 0.77sec.

Fig.15 shows the relationship between shear force and shear deformation of the rubber bearing. It shows both the experimental results and response analysis results. The compression side shows the results of the rubber bearing whose axial force increases as the horizontal deformation increases. On the contrary, the tension side shows the results of the rubber bearing whose axial force decreases as the horizontal deformation increases. Consequently, the results of compression side covered upward and the results of tension side covered downward even though the experimental results have same energy absorption. The results of response analysis don't have energy absorption because it is considered linear characteristics. It is also the same tendency by the axial force to the test results.

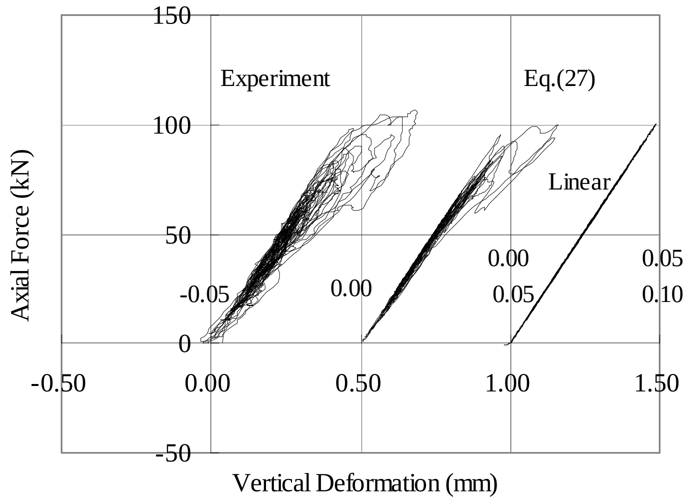

Fig.16 Vertical Deformation

The vertical stiffness

Fig.16 shows the result of axial stiffness. This figure also shows the results of two-response analysis, one is assumed that the vertical stiffness is affected by the horizontal deformation and another is assumed to be elastic. The test results show the energy absorption. When the horizontal deformation is large, the rocking moment and axial force is generally large in the compression side. Consequently, the vertical stiffness reduces and vertical deformation increases. The experimental results show this tendency. The response analysis results don't show the energy absorption because the rubber bearing is assumed to be elastic. But, the effect of axial force matches with the test results. From those results, it is shown that the axial deformation is underestimated if the horizontal dependency is not considered.

CONCLUSION

To gain an understanding of the force-deformation relationships of base-isolation rubber bearings with forced rotation angles at their top/bottom end and to clarify the effects of large axial force, a simple model is proposed. It coincides with Haringx's theory when the rubber is assumed to be elastic. The axial force dependency to the rotation stiffness is theoretically obtained. Also the vertical deformation is obtained when the rotation is theoretically considered.

The dependencies of horizontal deformation and axial force to the stiffness are obtained from the test results. It is confirmed that this model can be used when the axial dependency and horizontal dependency are considered simultaneously. The theoretical vertical deformation considering rotation is confirmed by the test results. Those proposed models are applied to a dynamic response analysis, and the results are confirmed by the shaking table test.

From those results, it is verified that the evaluation of the effects of rotation, large axial stress and large horizontal deformation become possible by the proposed models.

ACKNOWLEDGMENT

The program "DAISY" was revised by the authors for the response analysis conducted in this paper. The original one was developed in the research project " Research on base isolation techniques of nuclear facility in the next generation" held at the BRP in 1996-2001.

REFERENCES

1. Haringx J. A. “On Highly Compressible Helical Springs and Rubber Rods, and Their Application for Vibration-Free Mountings I”, Philips Research Reports, 1948, Vol.3, 401-449
2. Haringx J. A. “On Highly Compressible Helical Springs and Rubber Rods, and Their Application for Vibration-Free Mountings II”, Philips Research Reports, 1949, Vol.4, 48-80
3. Haringx J. A. “On Highly Compressible Helical Springs and Rubber Rods, and Their Application for Vibration-Free Mountings III”, Philips Research Reports, 1949, Vol.4, 206-220
4. Iizuka M, “Stiffness Matrix of Laminated Rubber Bearings, Formulation based on Haringx’s Theory”, Summaries of Technical Papers of Annual Meeting, Architectural Institute of Japan, 1995, B-2, 619-620 (in Japanese)
5. Fuller K.N.G, Muhr A.H. et al., “Studies at MRPRA Related to Isolation Bearings”, 11th SMiRT Post Conference Seminar on Seismic Structures, 295-328, Japan, 1991
6. Uryu M, Nishikawa T, “Study of Stiffness, Deformation and Ultimate Characteristics of Base-Isolated Rubber Bearings”, Journal of Structural and Construction Engineering, AIJ, No.479, 1961.1, 119-128 (in Japanese)
7. Kato Y, Miyama T, et al.,” An Experimental Study on the Rotational and Vertical Load-Carrying Characteristics of Rubber Bearings”, Proceedings of the 12th World Conference on Earthquake Engineering, Paper no. 1105. 2000, Auckland, New Zealand
8. Ohyama H, Miyama T, et al., “Performance Test of Rubber Bearing Against Rotation and Vertical Translation under the Shear Deflection”, Summaries of Technical papers of Annual Meeting, Architectural Institute of Japan, 1998, B-2, 541-542 (in Japanese)
9. Feng D, Kato Y, Miyama T, et al., “On Characteristics of Rubber Bearing Subject to Rotation.”, Summaries of Technical papers of Annual Meeting, Architectural Institute of Japan, 1999, B-2, 569-570 (in Japanese)
10. Fujita T., Fujita s., et al., “Experimental Study of Laminated Rubber Bearing for Earthquake Isolation of Buildings (1st Report, Static Tests for Rubber Bearings of 490kN Rated Load), Transactions of the Japan Society of Mechanical Engineers, 1987.1, Vol. 53, No.485, 71-76, Japan (in Japanese)
11. Miyama T, Feng D, Masuda K, et al., “Shaking Table Test of Various Seismic Isolation System Part 1”, Summaries of Technical papers of Annual Meeting, Architectural Institute of Japan, 2001, B-2, 591-592, (in Japanese)
12. Miyama T, Feng D, Masuda K, et al., “Shaking Table Test of Various Seismic Isolation System Part 2”, Summaries of Technical papers of Annual Meeting, Architectural Institute of Japan, 2001, B-2, 593-594, (in Japanese)